Journal of Power Sources 195 (2010) 604–609

Contents lists available at ScienceDirect

Journal of Power Sources

journal homepage: www.elsevier.com/locate/jpowsour

Short communication

Temperature effect on the graphite exfoliation in propylene carbonate based electrolytes

H.F. Xiang[a], C.H. Chen[a,b,*], J. Zhang[a], K. Amine[b]

[a] CAS Key Laboratory of Materials for Energy Conversion, Department of Materials Science and Engineering, University of Science and Technology of China, Anhui, Hefei 230026, China
[b] Chemical Technology Division, Argonne National Laboratory, 9700 South Cass Avenue, Argonne, IL 60439, USA

ARTICLE INFO

Article history:
Received 18 March 2009
Received in revised form 14 July 2009
Accepted 18 July 2009
Available online 28 July 2009

Keywords:
Graphite
Intercalation
Exfoliation
Lithium battery

ABSTRACT

Graphite exfoliation at a low potential has long been an issue for lithium-ion cells using a propylene carbonate (PC) based electrolyte. Two different mechanisms have been proposed in literature to explain this structural degradation. In this study, the initial lithium intercalation temperature is found to have a great impact on the extent of the graphite exfoliation. At an elevated temperature, the exfoliation can be largely suppressed and the irreversible capacity loss is reduced substantially. After the initial cycling at 50 °C, the graphite anode can be cycled in a PC-based electrolyte at room temperature without the exfoliation problem. It is also discovered that such a graphite anode gives rise to a specific capacity of over 372 mAh g^{-1} at 50 °C and a room temperature capacity higher than that of a graphite anode with the initial lithium intercalation at room temperature. This finding sheds a new light on the exfoliation mechanism. It may lead to a simple cycling procedure that allows us to make rechargeable lithium-ion batteries with better safety and higher capacity.

1. Introduction

The last decade of the past century has witnessed the rapid development and great commercial success of the technology of rechargeable lithium-ion batteries. Only by replacing metallic lithium with a carbonaceous material as the active anode material, have the lithium-ion batteries with a long cycle life and sufficient safety become reality [1]. The carbonaceous materials here include hard carbon with an amorphous or nano-crystalline structure, and graphite with a crystalline structure with parallel graphene layers connected by van der Waals force. As the active anode material, graphite is superior to hard carbon in that it shows smaller irreversible capacity loss and better cycleability. However, a graphite anode is usually only compatible with an ethylene carbonate (EC) based electrolyte. When contacting with a propylene carbonate (PC) based electrolyte, which is advantageous over the EC-based one for its higher low-temperature conductivity and better safety, the graphite anode may suffer from substantial exfoliation problem during the initial lithium intercalation step. Consequently, a PC-based electrolyte cannot be used in lithium-ion batteries with graphite as the anode unless some electrolyte additives [2–5] or metal coating on the graphite particles [6,7] are introduced. Two slightly different failure mechanisms, i.e., the solvent co-intercalation scenario [8,9] and surface defects scenario [10–13], are used to explain the exfoliation phenomenon. Probably for fear of the negative effects of an elevated-temperature cycling on the cell capacity [14–17], the initial cycling is always performed at room temperature. An elevated temperature is regarded undesirable for the formation cycles of a cell with the EC-based electrolyte [18]. In the case of a PC-based electrolyte, however, our study reveals some positive impacts of cell activation at an elevated temperature.

In this work, we have discovered that the initial lithium intercalation temperature has a critical impact on the behavior of graphite exfoliation in a PC-based electrolyte. This finding sheds a new light on the exfoliation mechanism and, further, it may lead to developing some special procedure of cell cycling that can prevent the anode exfoliation without the help of electrolyte additives.

2. Experimental

A synthetic graphite powder MAG10 (Hitachi Powdered Metals Co. Ltd.) was used as received in this study. The particle morphology of the graphite powder was investigated with a scanning electron microscope (KYKY-AMRAY 1000 B). Its particle size distribution was analyzed with a photo size analyzer (NSKC-1A). The crystal structure was studied by X-ray diffraction (Rigaku D/Max—rA, CuKα radiation).

* Corresponding author at: CAS Key Laboratory of Materials for Energy Conversion, Department of Materials Science and Engineering, University of Science and Technology of China, Anhui, Hefei 230026, China. Tel.: +86 551 3606971.
E-mail address: cchchen@ustc.edu.cn (C.H. Chen).

0378-7753/$ – see front matter © 2009 Elsevier B.V. All rights reserved.
doi:10.1016/j.jpowsour.2009.07.036

In order to make a graphite electrode laminate, a slurry containing 80 wt% MAG10 and 20 wt% polyvinylidene fluoride (PVDF) dispersed in 1-methyl-2-pyrrolidinone was cast onto a copper foil. After vacuum drying at 70 °C, the laminate was punched into discs (1.4 cm in diameter) and graphite/$LiPF_6$ (1 M)/Li CR2032 coin cells were assembled in an argon-filled glove box (MBraun Labmaster 130). The electrolyte solvent is either EC:DEC (1:1 by weight, DEC is diethyl carbonate), PC:EC:MEC (3:3:4, MEC is methyl ethyl carbonate) or PC:EC (7:3).

The cells were galvanostatically cycled at the current density of 0.2 mA cm^{-2} between 0 and 2 V on a multi-channel battery cycler. During the cell cycling, current interruption of every 30 s was programmed to measure the DC impedance. The first three cycles were performed at room temperature and 50 °C, respectively. The cells first cycled at 50 °C were also subsequently cycled at room temperature. Cyclic voltammetry (CHI660 Electrochemical Workstation) was also used to study the cells at these two temperatures with a potential scan rate of 0.2 mV s^{-1}. The surface chemistry of the MAG10 electrode after three cycles was characterized using a Bruker Vector-22 IR spectrophotometer equipped with a MIRacle™ single reflection HATR. The electrodes were obtained by opening the relative cells, which were charged to 3 V with lithium extracted, and all of the electrodes were washed with DMC (dimethyl carbonate) followed by the ATR-FTIR test.

3. Results and discussion

The scanning electron micrograph (SEM) of MAG10 graphite is shown in Fig. 1. The powder is composed of flaky particles mostly in the range of 1 to 20 μm. The measurement of particle size distribution indicates that the D10, D50 and D90 of this powder are 4.6, 10 and 21 μm, respectively, wherein D10, D50, and D90 represent particle diameters at 10%, 50% and 90% points on an accumulation curve of a particle size distribution when the total weight is 100%. The XRD pattern of MAG10 (Fig. 2) shows that it consists of mainly hexagonal 2H phase (AB stacking) and a small amount of rhombohedral 3R phase (ABC stacking). Due to the presence of crosslinking of graphene layers in the 3R phase, it is less sensitive than the 2H phase for solvent co-intercalation with lithium ions [19].

Fig. 3 shows the electrochemical cycling of a MAG10/Li cell in the electrolyte of 1 M $LiPF_6$ in EC:DEC (1:1). The charge–discharge curves (Fig. 3a) are typical of lithium intercalation–deintercalation of graphite electrode. Except for the first discharge step during which the solid-electrolyte-interface (SEI) layer is formed on the graphite surface, excellent cycling performance is observed for this cell. The first discharge capacity (366 mAh g^{-1}) is close to the theoretical value 372 mAh g^{-1}, and reversible capacity is around 325 mAh g^{-1} in the subsequent cycles with a coulombic efficiency over 99%. The irreversible capacity loss of about 40 mAh g^{-1} should be spent on the decomposition of electrolyte and the formation of the SEI layer [20–22]. The cell impedance, or specific-area-impedance (ASI) here (Fig. 3b) derived from the current

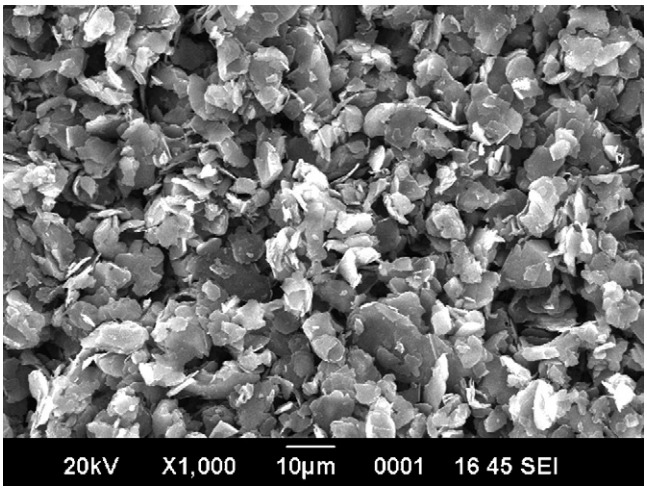

Fig. 1. Scanning electron micrograph of MAG10 graphite powder.

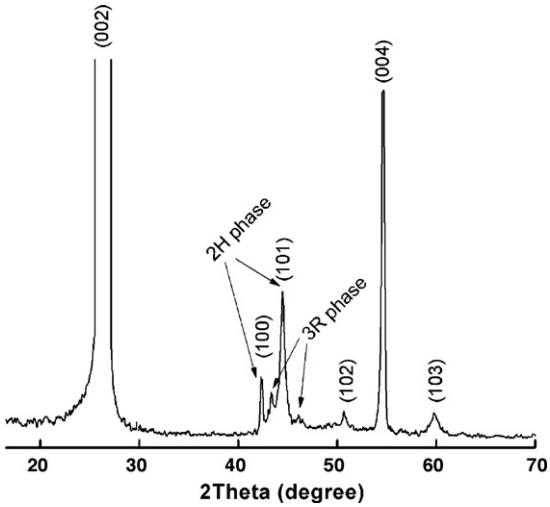

Fig. 2. X-ray diffraction pattern of MAG10 graphite powder. The indexed peaks are from 2H phase.

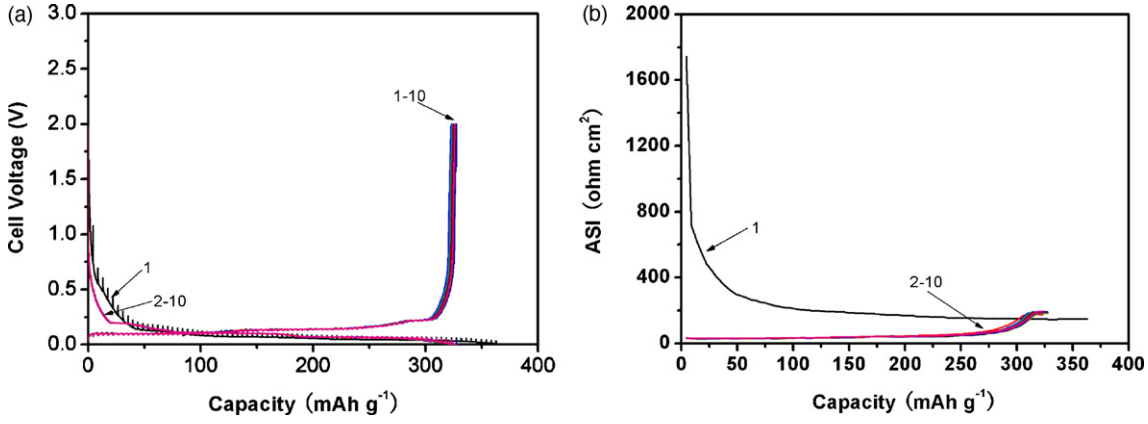

Fig. 3. Charge–discharge curves (a) and the area-specific-impedance (ASI) (b) of a MAG10/1 M $LiPF_6$ in EC:DEC (1:1)/Li cell at room temperature. The current density was 0.2 mA cm^{-2}.

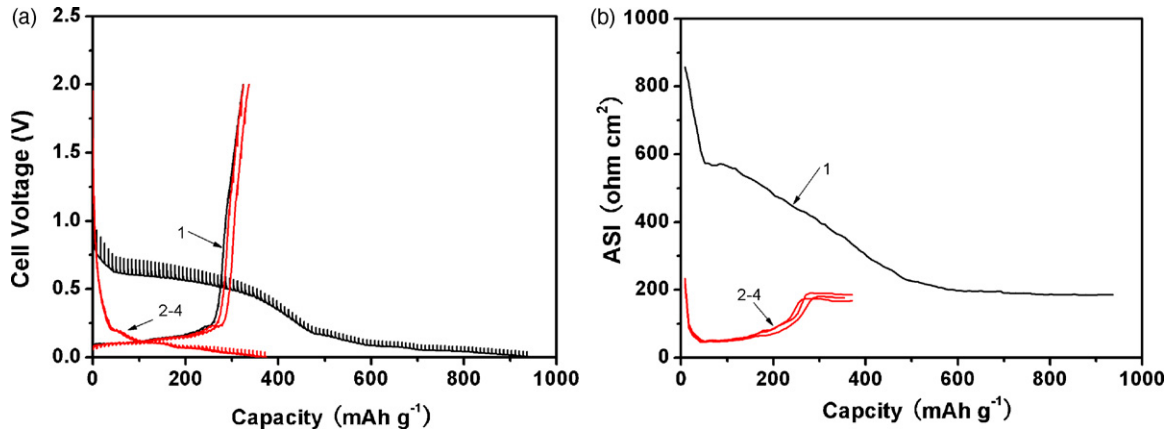

Fig. 4. Charge–discharge curves (a) and the area-specific-impedance (ASI) (b) of a MAG10/1 M $LiPF_6$ in PC:EC:MEC (3:3:4)/Li cell at room temperature. The current density was 0.2 mA cm^{-2}.

interruption measurement shows that relatively large impedance is observed in the first discharge step, particularly in the beginning period corresponding to the cell voltage change from about 3 to 0.2 V. This period is also for the formation of the SEI layer on the graphite surface as well as for the leaching-out of lithium ions from the fresh surface of lithium counter electrode. After this initial period, the cell impedance continues decreasing rather slowly until the end of the discharge step. During the subsequent cycles, the cell impedance is small, only about 30–50 ohm cm^2, during the lithium intercalation. Only when lithium has almost filled up the allowable sites between graphene layers, or x in C_6Li_x is close to 1, near the end of discharge steps, the cell impedance rises quickly. Note that the results of charge steps give the same relationship between the cell impedance and the lithium content in the graphite electrode.

Fig. 4 shows the electrochemical cycling of a MAG10/Li cell in the electrolyte of 1 M $LiPF_6$ in PC:EC:MEC (3:3:4) at room temperature. The voltage profiles (Fig. 4a) indicate that a substantial degree of graphite exfoliation takes place in the first discharge step from 0.9 to 0.25 V. The exfoliation leads to an irreversible capacity loss of about 500 mAh g^{-1}. Although the reversible charge capacity of the cell between 0 and 2 V still reaches about 325 mAh g^{-1}, the charge capacity between 0 and 0.25 V is only around 280 mAh g^{-1}.

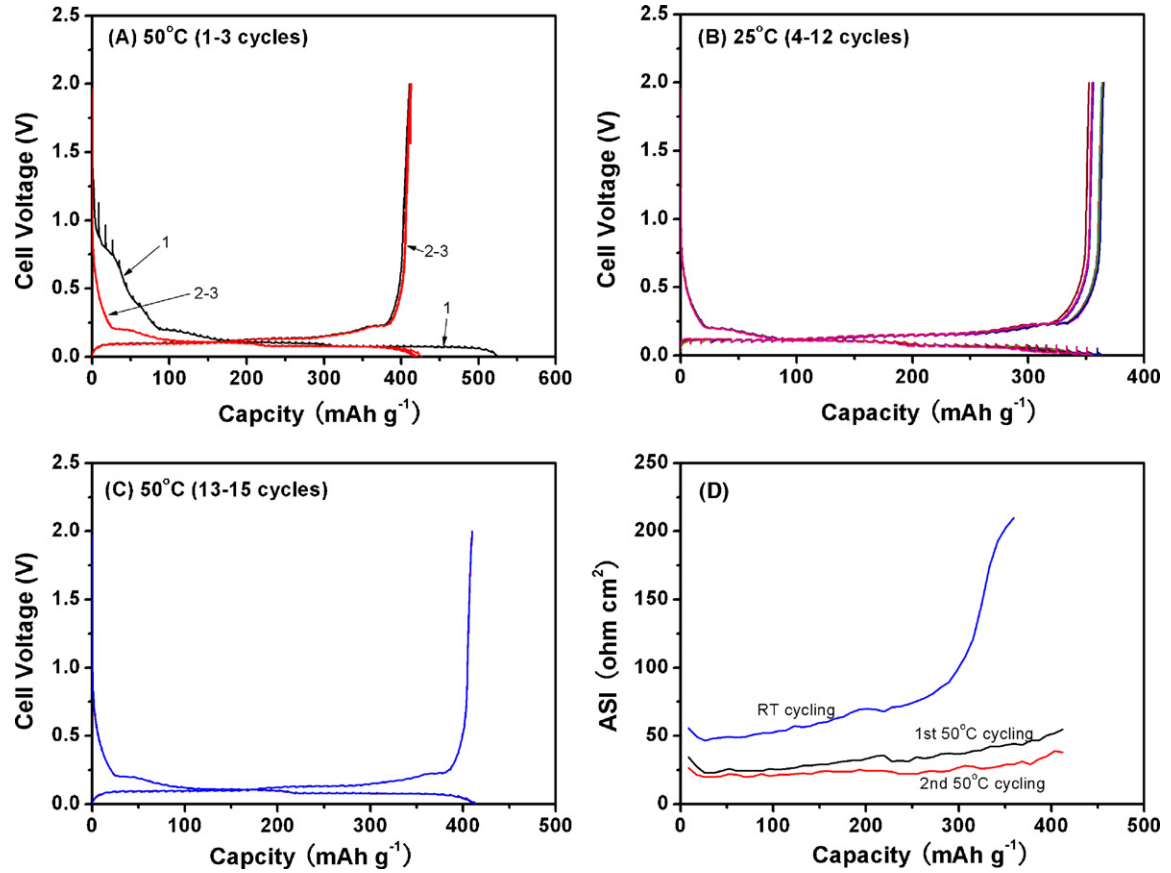

Fig. 5. Charge–discharge curves of a MAG10/1 M $LiPF_6$ in PC:EC:MEC (3:3:4)/Li cell first activated at 50 °C (a) then cycled at room temperature (b) and again at 50 °C (c). The current density was 0.2 mA cm^{-2}. The obtained ASI is combined in (d).

Besides, the coulombic efficiency of the cycling is only about 87%. Obviously, the graphite exfoliation in this 30% PC-based electrolyte has a detrimental influence on the cell performance. Thus, under similar conditions, MAG10 graphite in the present form cannot be used as the anode of lithium-ion cells. The impedance measurements (Fig. 4b) also show that the ASI associated with the graphite exfoliation is above 200 ohm cm^2, while it reduces to about 50 ohm cm^2 in the subsequent cycles.

When the formation cycles of the MAG10 graphite/Li cells in the 30% PC-based electrolyte are performed at 50 °C, we obtained significantly different results compared with the room temperature activation. An alternating-temperature cycling (ATC) procedure, i.e., first at 50 °C followed by room temperature and then 50 °C, was adopted (Fig. 5). Obviously, the graphite exfoliation is largely suppressed in the first discharge step at 50 °C (Fig. 5a). The SEI layer on the graphite surface must be formed at this step to prevent the graphite from further exfoliation in the subsequent cycles. It is interesting to find that this protective effect can be remained when the temperature is lowered to room temperature (Fig. 5b) and increased to 50 °C again (Fig. 5c). Due probably to the difference in ASI at the two temperatures (Fig. 5d), the reversible capacity at 50 °C is higher than that at room temperature. Therefore, the simple adoption of ATC procedure provides a way to use graphite as the anode of lithium-ion batteries with a PC-based electrolyte without the help of electrolyte additives or pre-coating the graphite powder.

Apart from the significant difference in the ability to suppress the graphite exfoliation, the formation cycles at 50 °C also gives rise to an increase in the reversible capacity (Fig. 6). Firstly, the reversible capacity at room temperature is around 363 mAh g^{-1}, considerably greater than 325 mAh g^{-1} obtained from the room temperature cycling of the 30% PC-electrolyte cell (Fig. 4) and even the non-PC-electrolyte cell (Fig. 3). Since the irreversible capacity loss is mainly attributed to the formation of SEI layer [20–22], this result suggests that less amount of SEI layer is formed at 50 °C cell activation. Secondly, its reversible capacity at 50 °C is around 412 mAh g^{-1}, which is, surprisingly, higher than the maximum theoretical value 372 mAh g^{-1} calculated by the well-known fully-lithiated state C_6Li. The voltage profiles (Figs. 5a and c) indicate that the dominant portion of this capacity, over 390 mAh g^{-1}, is obtained in the voltage range between 0 and 0.25 V. The reason behind this surprisingly large capacity is not very clear at this moment. It might suggest that, in addition to the traditional interlayer lithium storage model where every C_6 unit accommodates one lithium atom (LiC_6), another mechanism such as the lithium storage at graphite surface or graphene layer edges as proposed by Matsumura et al. [23] also takes place at the elevated temperature. Of course, further study is needed to disclose the real reason.

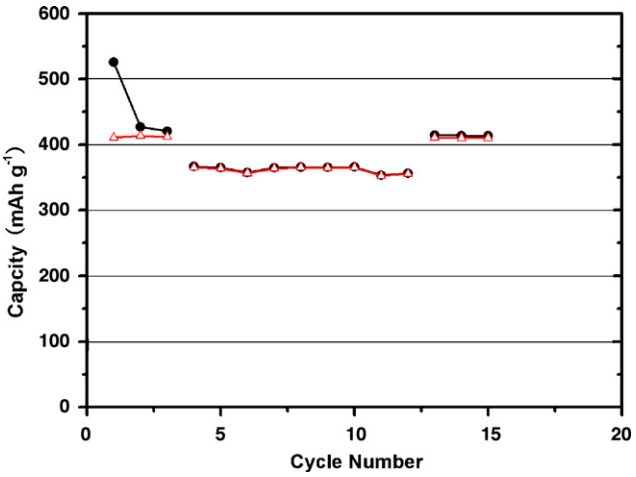

Fig. 6. Specific charge–discharge capacity of the same cell as for Fig. 5. The solid circles are for lithiation and open triangles for delithiation.

Cyclic voltammetry measurement (Fig. 7) has confirmed the suppression effect at 50 °C. At room temperature (Fig. 7a), the first lithium intercalation step gives rise to a broad and large reduction band between 0.9 and 0 V vs. Li^+/Li, which is typical of graphite exfoliation due to the reduction and decomposition of PC molecules [22]. At the anodic process, there is only an unconspicuous peak around 0.25 V, which is ascribed to lithium extraction from the graphite electrode. During the following scans, this anodic peak rises gradually, which suggests that an unstable SEI layer is formed in the first cathodic scan. Its composition and microstructure may be adjusted in the subsequent cycles to become a more stable SEI layer so that the electrode impedance decreases accordingly. In contrast to the room temperature cycling, an obvious cathodic peak from 1.0 to 0.6 V can be trusted in as a symbol of an SEI layer at 50 °C (Fig. 7b). Such a stable SEI layer can effectively suppress the graphite exfoliation and result in the higher reversibility of intercalation–deintercalation for Li^+. And the intercalation–deintercalation peaks (Fig. 7b) are markedly stronger than those in Fig. 7a, indicating a decrease in the cell impedance and an increase in the charge–discharge capacity as verified in Figs. 5 and 6.

Fig. 8 shows the SEMs of the different electrodes cycled three times at room temperature and 50 °C. It is obvious that the electrode cycled at 50 °C has relatively smooth surface (Fig. 8b), which suggest indirectly a compact and stable SEI layer is formed. But the

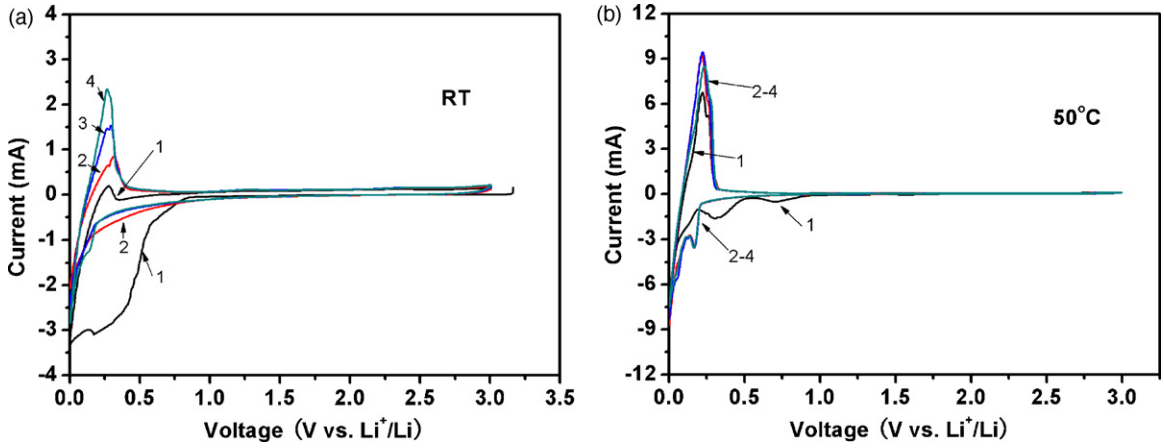

Fig. 7. Cyclic voltammograms of MAG10/1 M $LiPF_6$ in PC:EC:MEC (3:3:4)/Li cells at room temperature (a) and at 50 °C (b). The potential scan rate was 0.2 mV s^{-1}.

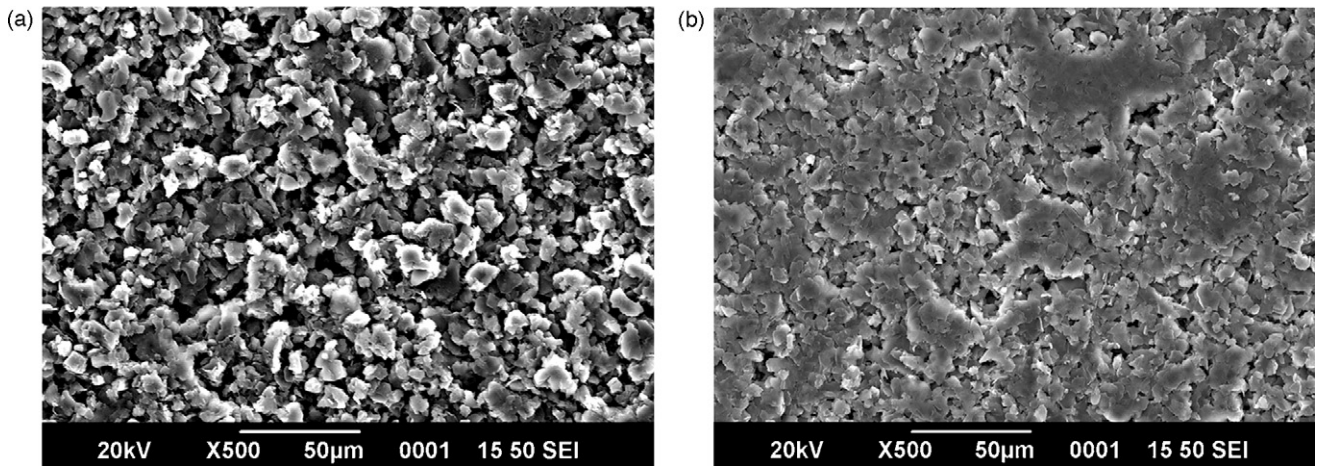

Fig. 8. Scanning electron micrographs of MAG10 graphite electrodes from MAG10/1 M $LiPF_6$ in PC:EC:MEC (3:3:4)/Li cells after cycled three times at room temperature (a) and at 50 °C (b).

electrode cycled at room temperature only has an inferior SEI layer deduced from the coarse surface (Fig. 8a), which is probably because the graphite exfoliation results in the larger surface area and hence more Li reacts with solvents on the interface. The surface chemistry of the electrodes was investigated by ATR-FTIR technology in Fig. 9. According to the previous reports [24,25], the peaks at 1503, 1426, and 865 cm^{-1} are characteristic peaks of Li_2CO_3, and the peaks at 1630, 1401, 1320, 820 cm^{-1} are attributed to lithium alkyl carbonate ($ROCO_2Li$) species. Hence it can be easily found that the SEI layer formed at room temperature contains more organic lithium alkyl carbonate ($ROCO_2Li$) species, but the layer formed at 50 °C is made up of more inorganic lithium carbonate component. This result is similar to that in the EC-based electrolyte [18], where Li_2CO_3 was more apt to be formed at the elevated temperature than $ROCO_2Li$. Compared to the organic species, inorganic lithium carbonate is facile to form the compact SEI layer, which effectively suppresses the graphite exfoliation caused by the surface defects as proposed by Aurbach et al. [11,12] and hence better cell performance at 50 °C is observed.

Nevertheless, with the increase of PC percentage in the solution, this suppression effect may not be observed. This is the case in the cells with a 70% PC-based electrolyte is used (Fig. 10).

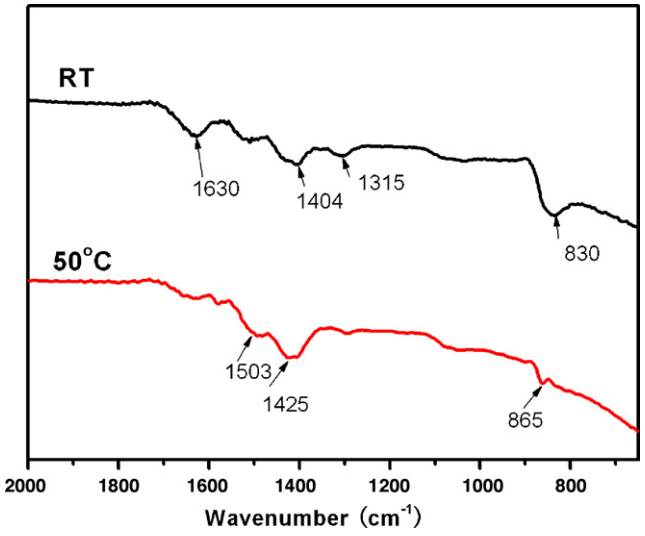

Fig. 9. The FTIR spectra of MAG10 graphite electrodes from MAG10/1 M $LiPF_6$ in PC:EC:MEC (3:3:4)/Li cells after cycled three times at room temperature (25 °C) and at 50 °C.

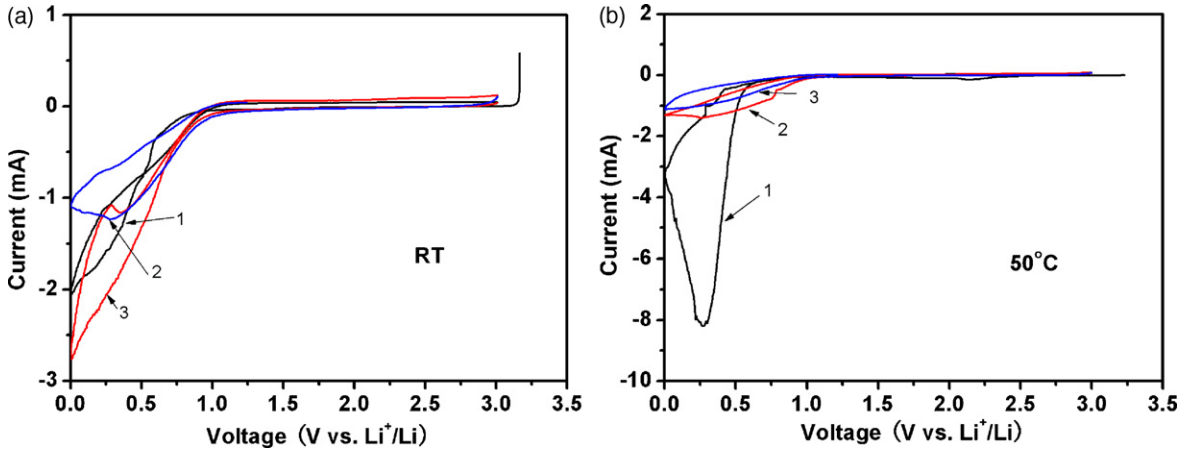

Fig. 10. Cyclic voltammograms of MAG10/1 M $LiPF_6$ in PC:EC (7:3)/Li cells at room temperature (a) and at 50 °C (b). The potential scan rate was 0.2 mV s^{-1}.

4. Conclusions

The temperature of initial lithium intercalation into a graphite electrode has a critical effect on the graphite exfoliation and even the reversible intercalation–deintercalation capacity in graphite/Li cells with PC-based electrolytes. For those cells using a PC-based cell (up to 30 wt% PC), it is discovered that the exfoliation of the graphite electrode can be greatly suppressed by performing the first formation cycles at 50 °C. This suppression effect is remained when the cells are cycled at room temperature again after the 50 °C formation cycles.

Acknowledgements

This work was partially supported Education Department of Anhui Province (grant no. KJ2009A142) and partially supported by a grant W-31-109-Eng-38 from U.S. We are also grateful to Dr. C.S. Johnson from Argonne National Lab for his help at the beginning of this study.

References

[1] T. Nagaura, K. Tozawa, Prog. Batt. Solar Cells 9 (1990) 209.
[2] G.H. Wrodnigg, J.O. Besenhard, M. Winter, J. Electrochem. Soc. 146 (1999) 470.
[3] Y. Ein-Eli, S.R. Thomas, V.R. Koch, J. Electrochem. Soc. 143 (1996) L195.
[4] P. Ghimire, H. Nakamura, M. Yoshio, H. Yoshitake, K. Abe, Electrochemistry 71 (2003) 1084.
[5] G.E. Blomgren, J. Power Sources 119 (2003) 326.
[6] P. Yu, J.A. Ritter, R.E. White, B.N. Popov, J. Electrochem. Soc. 147 (2000) 1280.
[7] W. Lu, V.S. Donepudi, J. Prakash, J. Liu, K. Amine, Electrochim. Acta 47 (2002) 1601.
[8] J.O. Besenhard, M. Winter, J. Yang, W. Biberacher, J. Power Sources 54 (1995) 228.
[9] G.C. Chung, H.J. Kim, S.I. Yu, S.H. Jun, J.W. Choi, M.H. Kim, J. Electrochem. Soc. 147 (1995) 4391.
[10] E. Peled, D. Golodnitsky, C. Menachem, D. Bar-Tow, J. Electrochem. Soc. 145 (1998) 3482.
[11] D. Aurbach, M.D. Levi, E. Levi, A. Schechter, J. Phys. Chem. B 101 (1997) 2195.
[12] D. Aurbach, B. Markovsky, I. Weissman, E. Levi, Y. Ein-Eli, Electrochim. Acta 45 (1999) 67.
[13] D. Aurbach, M. Koltypin, H. Teller, Langmuir 18 (2002) 9000.
[14] P. Arora, R.E. White, M. Doyle, J. Electrochem. Soc. 145 (1998) 3647.
[15] M.N. Richard, J.R. Dahn, J. Electrochem. Soc. 146 (1999) 2068.
[16] T. Zheng, A.S. Gozdz, G.G. Amatucci, J. Electrochem. Soc. 146 (1999) 4014.
[17] A. Du Pasquier, F. Disma, T. Bowmer, A.S. Gozdz, G. Amatucci, J.M. Tarascon, J. Electrochem. Soc. 145 (1998) 472.
[18] S.B. Lee, S.I. Pyun, Carbon 40 (2002) 2333.
[19] W. Kohs, H.J. Santner, F. Hofer, H. Schrottner, J. Doninger, I. Barsukov, H. Buqa, J.H. Albering, K.C. Moller, J.O. Besenhard, M. Winter, J. Power Sources 119 (2003) 528.
[20] M. Winter, P. Novak, A. Monnier, J. Electrochem. Soc. 145 (1998) 428.
[21] D. Bar-Tow, E. Peled, L. Burstein, J. Electrochem. Soc. 146 (1999) 824.
[22] G.C. Chung, S.H. Jun, K.Y. Lee, M.H. Kim, J. Electrochem. Soc. 146 (1999) 1664.
[23] Y. Matsumura, S. Wang, J. Mondori, Carbon 33 (1995) 1457.
[24] D. Aurbach, K. Gamolsky, B. Markovsky, Gofer, Schmidt, U. Heider, Electrochim. Acta 47 (2002) 1423.
[25] X. Xie, L. Chen, W. Sun, J. Xie, J. Power Sources 174 (2007) 784.